Damage buildup in GaN under ion bombardment

S. O. Kucheyev,* J. S. Williams, and C. Jagadish

Department of Electronic Materials Engineering, Research School of Physical Sciences and Engineering,
The Australian National University, Canberra, ACT 0200, Australia

J. Zou

Electron Microscope Unit and Australian Key Center for Microscopy and Microanalysis, The University of Sydney,
Sydney, NSW 2006, Australia

G. Li

LED Expert Corporation, No. 9, Ta-Yio 1st Street, Ta-Fa Industrial District, Kaohsiung County, Taiwan, Republic of China

The damage buildup until amorphization in wurtzite GaN films under keV light (^{12}C) and heavy (^{197}Au) ion bombardment at room and liquid nitrogen (LN$_2$) temperatures is studied by Rutherford backscattering/ channeling (RBS/C) spectrometry and transmission electron microscopy (TEM). The effect of beam flux on implantation damage in GaN is reported. A marked similarity between damage buildup for light and heavy ion bombardment regimes is observed. The results point to substantial dynamic annealing of irradiation defects even during heavy ion bombardment at LN$_2$ temperature. Amorphization starts from the GaN surface with increasing ion dose for both LN$_2$ and room-temperature bombardment with light or heavy ions. A strong surface defect peak, seen by RBS/C, arises from an amorphous layer at the GaN surface, as indicated by TEM. The origin of such an amorphous layer is attributed to the trapping of mobile point defects by the GaN surface, as suggested by the flux behavior. However, in the samples implanted with light ions to low doses (1 $\times 10^{15}$ cm^{-2}), no amorphous layer on the GaN surface is revealed by TEM. Damage buildup is highly sigmodal for LN$_2$ temperature irradiation with light or heavy ions. Formation of planar defects in the crystal bulk is assumed to provide a ''nucleation site'' for amorphization with increasing ion dose during irradiation at LN$_2$ temperature. For room-temperature bombardment with heavy ions, the damage in the GaN bulk region saturates at a level lower than that of the amorphous phase, as measured by RBS/C, and amorphization proceeds from the GaN surface with increasing ion dose. For such a saturation regime at room temperature, implantation damage in the bulk consists of point-defect clusters and planar defects which are parallel to the basal plane of the GaN film. Various defect interaction processes in GaN during ion bombardment are proposed to explain the observed, somewhat unexpected behavior of disorder buildup.

I. INTRODUCTION

For much of the past decade, extensive studies of GaN have demonstrated amazing success leading to the fabrication of a range of both electronic and photonic devices.[1] However, given the present understanding of its properties and processes taking place during various technological steps, GaN is still far from being considered as a mature semiconductor material. In particular, the data reported in the literature on damage processes in GaN under ion bombardment are still rather limited and far from being understood despite the technological importance of studies on implantation-produced disorder in GaN. For example, ion implantation can be applied for selective-area doping and dry-etching of GaN. Because device performance depends on defect type and concentration, systematic studies of ion beam damage in GaN represent an example of not only a physically interesting research subject but also a study that may have significant implications for the fast developing GaN industry.

Up to now, few detailed studies have been reported on the structural characterization of disorder buildup in GaN under ion bombardment.[2–9] This situation is surprising since such studies often give an insight into the important properties of the defects produced by an ion beam. For example, information on the mobility and effective lifetimes of defects, defect clustering efficiency, and on the influence of interfaces on mobile defects can often be obtained from an analysis of damage buildup under ion irradiation.

Given the current understanding of ion beam damage processes in mature semiconductor materials such as Si and GaAs, one can select two limiting cases based on the characteristics of the collision cascades generated by energetic ions penetrating through a crystal.[10] These two cases are bombardment by light and heavy ions relative to the masses of the host atoms of the material under bombardment. In the case of light ions, collision cascades are very dilute and consist mostly of simple point defects such as vacancies and interstitials. In the case of heavy ions, where the nuclear energy loss rate is large, it is generally believed that each ion generates a dense collision cascade which, upon very fast quenching, can often result in an amorphous zone.[11] Bombardment by intermediate mass ions represents a combination of these two limiting cases.

Neither light nor heavy ion-induced damage buildup studies in GaN have been reported in the literature. Detailed

studies of amorphization behavior with increasing ion dose have been reported only for bombardment of GaN with Si,[2] Ar,[6] and Ca (Ref. 6) ions at liquid nitrogen (LN$_2$) temperature. The effects of implantation temperature and beam flux on the amorphization behavior of GaN have not been reported even for bombardment with these intermediate mass ions.

In this paper, we report on the results of our systematic study of structural damage in GaN under ion bombardment. We report here the influence of implant conditions on amorphization behavior of GaN during both light (^{12}C) and heavy ion (^{197}Au) bombardment. Rutherford backscattering/channeling (RBS/C) spectrometry was used to monitor gross lattice disorder, while cross-sectional transmission electron microscopy (TEM) was applied to identify the nature of the defects produced by an ion beam. The results point to a marked similarity between damage buildup for light and heavy ion bombardment regimes. However, some differences between these two regimes have also been observed. Based on the experimental results, we propose an explanation for the complex damage accumulation observed in GaN under ion bombardment.

II. EXPERIMENT

The wurtzite GaN layers used in this study were ~ 2 μm thick, epitaxially grown on c-plane sapphire substrates by metalorganic chemical vapor deposition (MOCVD) in a rotating disk reactor at LED Expert Corporation. Implantation with 40 keV ^{12}C and with 100, 300, and 450 keV ^{197}Au ions was done at LN$_2$ and RT over a wide dose range. Implantation with 40 keV ^{12}C and 100 keV ^{197}Au ions was carried out using the ANU 180 kV ion implanter. The ANU 1.7 MV tandem accelerator (NEC, 5SDH) was used for the bombardment by higher energy ions. During implantation, samples were tilted by $\sim 7°$ relative to the incident ion beam to avoid channeling. An average scanned ion beam flux was kept constant during implantation to different doses by ions with the same energy and mass to study damage buildup. Additional implantation was performed at different beam fluxes.

For some samples, prior to ion bombardment, silicon oxide (SiO$_x$) or silicon nitride (Si$_x$N$_y$) capping layers (~ 300 Å thick) were deposited on the GaN surface at temperatures of 100 °C (in the case of SiO$_x$) and 300 °C (in the case of Si$_x$N$_y$) using an Oxford Plasmalab 80 plasma enhanced chemical vapor deposition (PECVD) system at the ANU. The deposition was carried out in order to prevent decomposition of GaN during ion bombardment. Atomic force microscopy (AFM) was used to monitor the quality of deposited capping layers.

After implantation, samples were analyzed *ex situ* by RBS/C with 1.8 MeV ^{4}He$^+$ ions incident along the [0001] direction and backscattered into detectors at $\sim 170°$ and 98° relative to the incident beam direction. The latter glancing-angle detector was used to provide enhanced depth resolution for examining near-surface damage accumulation. Cross-sectional TEM specimens were prepared by Ar$^+$ ion beam thinning using a Gatan precision ion polishing system operating at 3 keV. These TEM specimens were investigated in a Philips CM12 TEM operating at 120 keV.
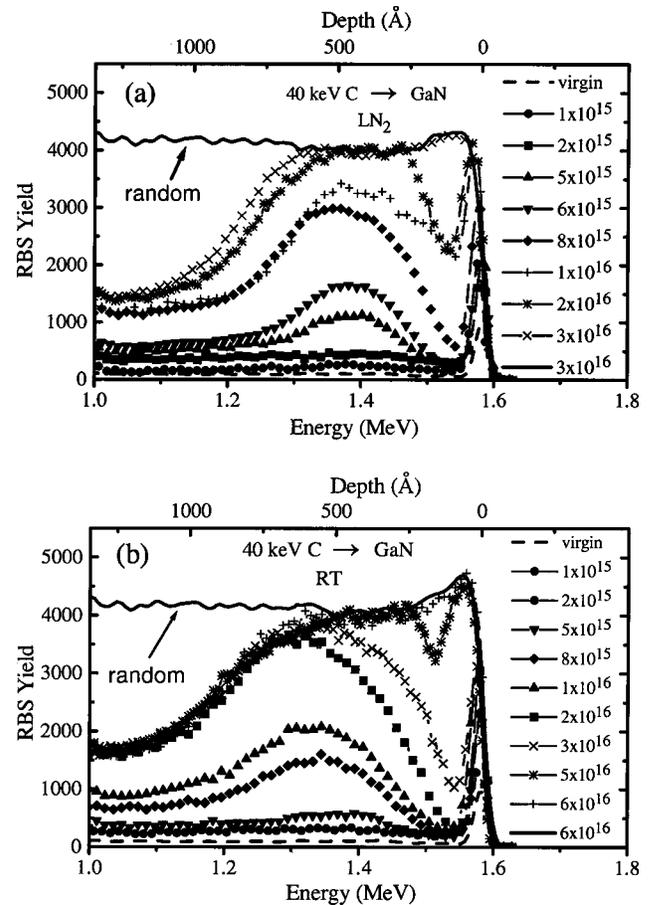

FIG. 1. RBS/C spectra showing the damage buildup for 40 keV C ion bombardment of GaN at LN$_2$ (a) and RT (b) with a beam flux of 1.4×10^{13} cm^{-2} s^{-1}. Implantation doses (in cm^{-2}) are indicated in the figure.

III. RESULTS

A. Bombardment with 40 keV C ions

Figure 1 shows RBS/C spectra that illustrate the damage buildup in GaN with an increasing dose of 40 keV C ions implanted with a beam flux of 1.4×10^{13} cm^{-2} s^{-1} at LN$_2$ [Fig. 1(a)] and RT [Fig. 1(b)]. A number of features of these spectra, which show damage in the Ga sublattice, are of interest. First, the distorted shape of the RBS/C spectra for GaN implanted to high doses ($>2 \times 10^{16}$ cm^{-2}) is due to the formation of a C$_x$Ga$_y$N$_z$ alloy with an increasing dose of C ions.[12] This effect is also illustrated in Fig. 2, which shows that, with increasing ion dose, the aligned RBS/C spectra exhibit a complex behavior with a general trend of *reduction* in the yield for high doses ($>5 \times 10^{16}$ cm^{-2}). It is interesting that, relative to the energy scale, the depth scale also changes with increasing dose due to the changes in the energy losses of the analyzing 1.8 MeV He$^+$ ions. Such a complex behavior is a result of the introduction into the GaN lattice of a high concentration of ^{12}C atoms, which are much lighter than ^{70}Ga. As shown by us previously,[9] the preferential loss of nitrogen during high-dose ion bombardment also influences the RBS/C yield in the near-surface region. Figure 2 clearly illustrates a potential difficulty of studying amorphization in GaN under light ion bombardment when very high doses are required for amorphization.
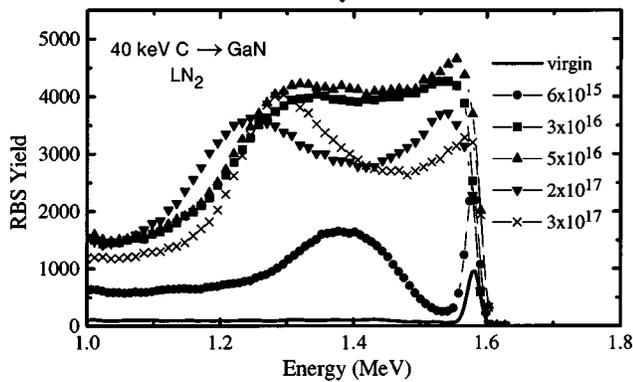
FIG. 2. RBS/C spectra of GaN implanted to high doses with 40 keV C ions at LN_2 temperature with a beam flux of 1.4×10^{13} cm^{-2} s^{-1}. Implantation doses (in cm^{-2}) are indicated in the figure.

Also seen from Fig. 1 is an apparent small shift of the maximum of the bulk defect peak to lower backscattering energies with increasing level of lattice disorder. This shift has been attributed to the difference in the energy loss of analyzing 1.8 MeV He$^+$ ions incident along channeling and random directions.[13] It should be noted that the depth scales in the RBS/C spectra reported in this paper have been calculated with the stopping powers of Ga and N in an amorphous matrix. Therefore, the depth scales should be more accurate for the spectra with high damage levels, where the error resulting from the different stopping power in a channeling direction should be small. This has been discussed in more detail elsewhere.[13]

Another feature seen from Fig. 1 is that an increase in the implantation temperature from LN_2 to RT appreciably reduces implantation damage. Although this trend is not unexpected, the magnitude of the temperature effect on post-implantation damage is of more interest. The results from Fig. 1 do not indicate a very strong effect of the temperature on the gross amount of post-implantation disorder in GaN under the implant conditions of this study. However, it is reasonable to expect a much stronger effect of implantation temperature on damage for some beam flux values different from the one used in this study (1.4×10^{13} cm^{-2} s^{-1}). Indeed, for mature semiconductor materials (Si and GaAs) for some implantation regimes with substantial dynamic annealing (i.e., at elevated temperatures), it has been shown that the effect of implantation temperature on post-implantation disorder can be strong, but the magnitude of the effect can appreciably depend on beam flux (see, for example, Refs. 14 and 15).

The next important feature from Fig. 1 is that the shape of the measured damage profiles significantly departs from an expected Gaussian-like defect profile calculated based only on the nuclear energy loss processes using, for example, the TRIM code.[16] Two peaks in the experimental damage distribution are clearly seen, corresponding to surface and bulk peaks of disorder. The bulk peak close to the depth of the maximum nuclear energy loss (~ 500 Å) is not unexpected. However, as reported by us previously,[9] an unusually strong surface peak of disorder in GaN bombarded under a wide range of implant conditions is somewhat surprising. Our previous results[9] indicated that nitrogen loss was not the main
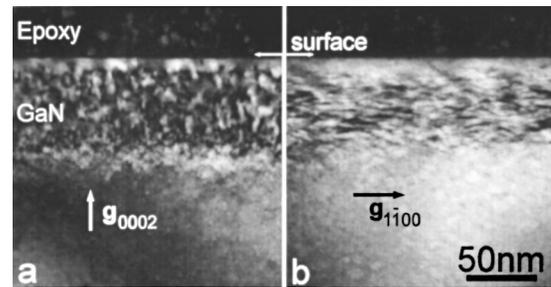

FIG. 3. Cross-sectional dark-field TEM images [(a) $\mathbf{g} = 0002*$ and (b) $\mathbf{g} = 1\bar{1}00*$] of the GaN epilayers bombarded with 40 keV C ions with a beam flux of 1.4×10^{13} cm^{-2} s^{-1} to a dose of 8×10^{15} cm^{-2} at LN_2 temperature.

reason for the appearance of a strong surface peak and suggested that the GaN surface acted as a strong sink for migrating point defects. This effect is discussed in more detail below.

Figure 3 shows dark-field TEM images taken from GaN implanted with 40 keV C ions with a beam flux of 1.4×10^{13} cm^{-2} s^{-1} to a dose of 8×10^{15} cm^{-2} at LN_2 temperature. The RBS/C spectrum of the same sample is shown by diamonds in Fig. 1(a). The TEM micrograph shown in Fig. 3(a) ($\mathbf{g} = 0002*$) indicates the presence of point-defect clusters in the implanted region (up to ~ 900 Å from the GaN surface). In addition, the image with $\mathbf{g} = 1\bar{1}00*$ shown in Fig. 3(b) reveals some planar defects present in the bulk defect peak region. These planar defects are parallel to the basal plane of the GaN film. Although the region between bulk and surface defect peaks is free from planar defects [see Fig. 3(b)], a small concentration of point-defect clusters is present in this region, as indicated by Fig. 3(a). Therefore, these TEM data are in good agreement with the damage depth profile measured by RBS/C [Fig. 1(a)].

Selected samples have been studied by cross-sectional TEM with the electron beam precisely parallel to the GaN surface to eliminate edge effects on the contrast of the near-surface region. Figure 4(a) shows such a bright-field image of the same sample depicted in Fig. 3. A thin layer of amorphous material on the GaN surface is clearly seen. This layer has a different contrast to that of the glue and of the crystalline GaN. TEM investigation by switching between bright-field imaging and dark-field imaging indicates that this layer is amorphous. This finding is also consistent with the RBS/C
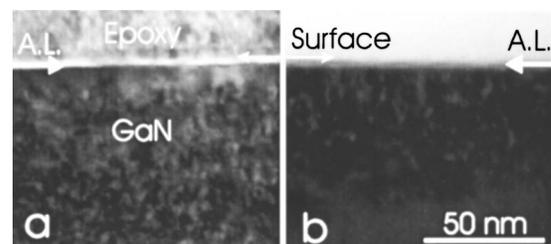

FIG. 4. (a) Cross-sectional bright-field TEM image taken from the same GaN sample depicted in Fig. 3. (b) Cross-sectional bright-field TEM image of GaN implanted with 100 keV Au ions with a beam flux of 1.4×10^{13} cm^{-2} s^{-1} to a dose of 3×10^{14} cm^{-2} at LN_2 temperature. Amorphous layers (labeled as A.L.) on the GaN surface are clearly demonstrated.
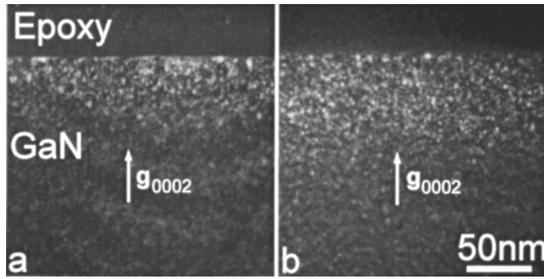
FIG. 5. Cross-sectional weak-beam TEM images ($\mathbf{g}=0002^*$ with $\mathbf{g}/6.1\mathbf{g}$ imaging condition) of the GaN epilayers bombarded with 40 keV C ions with a beam flux of $1.4\times10^{13}\,cm^{-2}\,s^{-1}$ to a dose of $1\times10^{15}\,cm^{-2}$ at LN$_2$ (a) and RT (b).

yield reaching the random level at the surface, as measured with the glancing-angle detector geometry. For comparison, Fig. 4(b) shows a bright-field micrograph of a sample implanted with Au ions, which is described later.

Figure 5 shows $\mathbf{g}=0002^*$ (with $\mathbf{g}/6.1\mathbf{g}$ imaging condition) weak-beam TEM images taken from samples implanted with 40 keV C ions with a beam flux of $1.4\times10^{13}\,cm^{-2}\,s^{-1}$ to a dose of $1\times10^{15}\,cm^{-2}$ at LN$_2$ [Fig. 5(a)] and RT [Fig. 5(b)]. Figure 5 indicates that, for such a low-dose implantation[17] ($1\times10^{15}\,cm^{-2}$), RT bombardment produces a similar type of residual damage to irradiation at LN$_2$ temperature. In addition, a comparison of RBS/C spectra of these two samples [see Figs. 1(a) and 1(b)] suggests a higher damage level in the RT implanted sample. The RBS/C yield
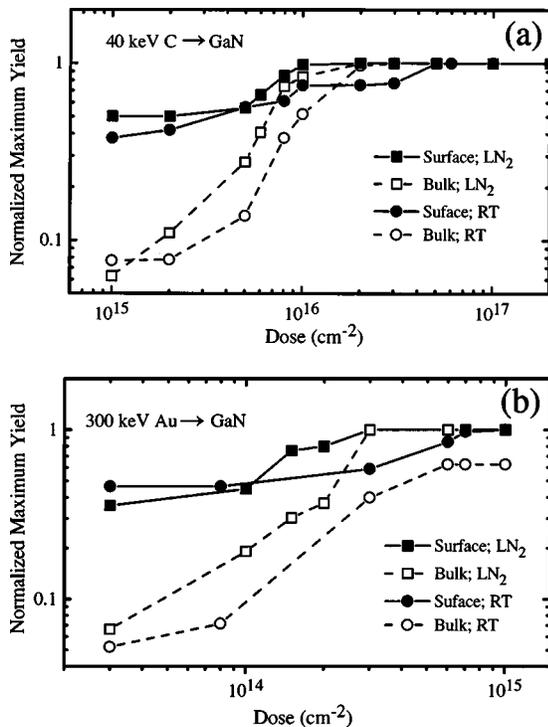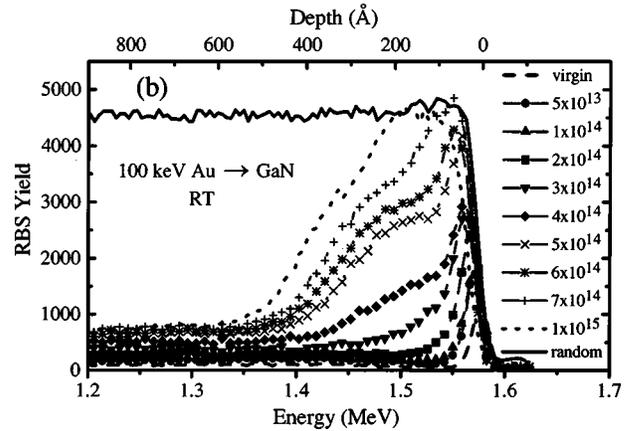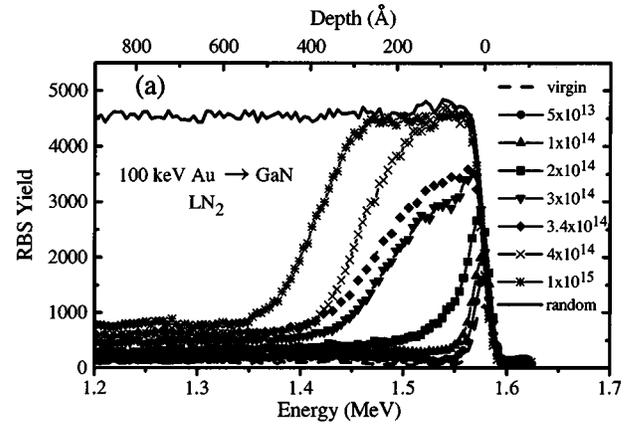

FIG. 7. RBS/C spectra showing the damage buildup for 100 keV Au ion bombardment of GaN at LN$_2$ (a) and RT (b) with a beam flux of $1.4\times10^{13}\,cm^{-2}\,s^{-1}$. Implantation doses (in cm^{-2}) are indicated in the figure.

of the sample implanted at RT is higher than that of the sample bombarded at LN$_2$ temperature to the same dose of $1\times10^{15}\,cm^{-2}$.

Figure 6(a) shows the magnitudes of the surface and bulk defect peaks, taken from Fig. 1, as a function of the dose of 40 keV C ions implanted at LN$_2$ and RT. The peak levels have been normalized to the random level for each dose to take into account the effect of high-dose implantation on the random yield. It is clearly seen from Fig. 6(a) that the damage buildup in GaN is highly sigmodal for the case of light ion bombardment. This behavior is consistent with the results of LN$_2$ temperature bombardment of GaN with intermediate mass ions [Si,[2] Ar,[6] and Ca (Ref. 6)]. Such a sigmodality represents a characteristic feature of nucleation-limited damage buildup, as discussed in more detail below.

FIG. 6. Dose dependence of the magnitudes of the bulk and surface defect peaks for 40 keV C ion bombardment at LN$_2$ and RT with a beam flux of $1.4\times10^{13}\,cm^{-2}\,s^{-1}$ (a) and for 300 keV Au ion bombardment at LN$_2$ temperature with a beam flux of $3.1\times10^{12}\,cm^{-2}\,s^{-1}$ and at RT with a beam flux of $4.4\times10^{12}\,cm^{-2}\,s^{-1}$ (b). The peak levels have been normalized to the random level.

B. Bombardment with 100 keV Au ions

Figure 7 shows RBS/C spectra that illustrate the damage buildup in GaN with an increasing dose of 100 keV Au ions implanted with a beam flux of $1.4\times10^{13}\,cm^{-2}\,s^{-1}$ at LN$_2$ [Fig. 7(a)] and RT [Fig. 7(b)]. A comparison of Figs. 7(a) and 7(b) reveals quite different damage buildup behavior with increasing the dose of 100 keV Au ions for LN$_2$ and RT bombardment regimes. Indeed, for LN$_2$ temperature irradiation, for doses up to $\sim2\times10^{14}\,cm^{-2}$, Fig. 7(a) shows an accumulation of damage preferentially at the GaN surface,
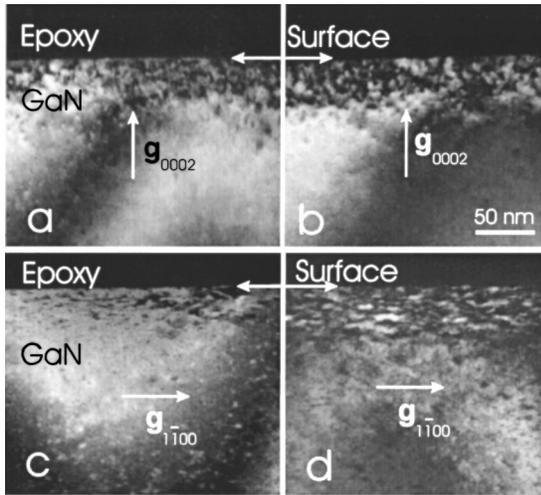
FIG. 8. Cross-sectional dark-field TEM images [(a),(b) **g** =0002*] and (c),(d) **g**=1$\bar{1}$00*] of the GaN epilayers bombarded with 100 keV Au ions with a beam flux of 1.4×10^{13} cm^{-2} s^{-1} to doses of 2×10^{14} cm^{-2} (a),(c) and 3×10^{14} cm^{-2} (b),(d) at LN$_2$ temperature.

away from the maximum of the nuclear energy loss profile. Then, in the dose range from $\sim 2 \times 10^{14}$ cm^{-2} to 4×10^{14} cm^{-2}, damage in the GaN bulk region (~ 150 Å from the GaN surface) exhibits a very rapid increase from a very low level to apparent amorphization, as indicated by the RBS/C yield reaching the random level. This rapid disorder buildup results in a strong sigmodality of the damage-dose function, as discussed in more detail below. In contrast to LN$_2$ temperature, bombardment at RT does not result in such a fast growth of damage in the bulk region with increasing ion dose [see Fig. 7(b)]. Instead, damage in the bulk region saturates below the random level, and amorphization appears to proceed layer-by-layer from the GaN surface, as indicated by RBS/C spectra shown in Fig. 7(b).

Figure 8 shows dark-field TEM images taken from GaN implanted with 100 keV Au ions with a beam flux of 1.4×10^{13} cm^{-2} s^{-1} to doses of 2×10^{14} cm^{-2} [Figs. 8(a) and 8(c)] and 3×10^{14} cm^{-2} [Figs. 8(b) and 8(d)] at LN$_2$ temperature. Images taken under the **g**=0002* condition [Figs. 8(a) and 8(b)] indicate the presence of point-defect clusters in the implanted regions (up to ~ 300 Å from the GaN surface), while images taken under the **g**=1$\bar{1}$00* condition [Figs. 8(c) and 8(d)] reveal some planar defects. The concentration of these planar defects, which are parallel to the basal plane of the GaN film, increases with increasing ion dose, as seen from a comparison of Figs. 8(c) and 8(d). A similar band of planar defects has been observed in GaN bombarded with light ions [see Fig. 3(b)].

Shown in Fig. 4(b) is a bright-field TEM image taken from the GaN sample shown in Figs. 8(b) and 8(d). This image was taken under the same conditions as the image from Fig. 4(a). The similarity between these two images for light and heavy ions is clear. Both exhibit thin surface amorphous layers and defect clusters in the bulk. This result suggests that ion bombardment with both light and heavy ions leads to the formation of a thin amorphous layer on the GaN surface. However, for 100 keV Au ion bombardment, the bulk damage profile is too shallow for the bulk defect peak
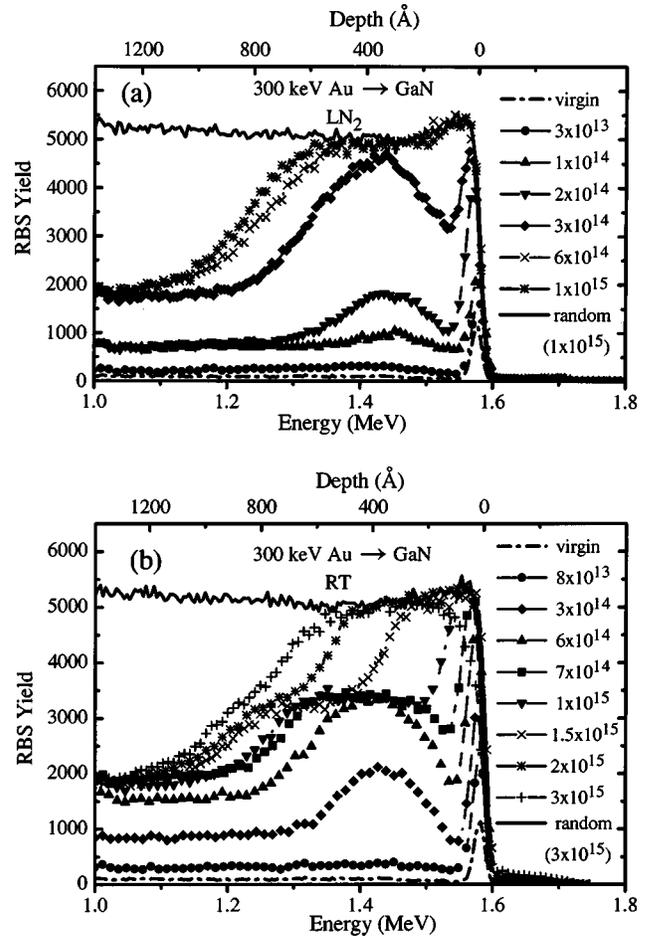

FIG. 9. RBS/C spectra showing the damage buildup for 300 keV Au ion bombardment of GaN at LN$_2$ temperature with a beam flux of 3.1×10^{12} cm^{-2} s^{-1} (a) and at RT with a beam flux of 4.4×10^{12} cm^{-2} s^{-1} (b). Implantation doses (in cm^{-2}) are indicated in the figure.

and a thin amorphous layer to be separated in the RBS/C spectra, even for the glancing-angle detector geometry used in this study. Therefore, a higher energy of gold ions has been used, as presented below.

C. Bombardment with 300 keV Au ions

Shown in Fig. 9 are RBS/C spectra illustrating damage accumulation in GaN with a dose of 300 keV Au ions implanted at LN$_2$ temperature with a beam flux of 3.1×10^{12} cm^{-2} s^{-1} [Fig. 9(a)] and at RT with a beam flux of 4.4×10^{12} cm^{-2} s^{-1} [Fig. 9(b)]. Compared to 100 keV Au bombardment, in this case the RBS/C depth resolution is sufficient for the bulk and surface peaks of disorder to be separated in the spectra. A comparison of Figs. 7 and 9 shows that the main features of damage buildup behavior do not change upon increasing the energy of Au ions from 100 to 300 keV. One can see the same highly sigmodal damage buildup for LN$_2$ temperature bombardment [Fig. 9(a)] and a pronounced effect of damage saturation in the bulk region for implantation at RT [Fig. 9(b)]. These effects are also illustrated in Fig. 6(b), which shows the magnitudes of the surface and bulk defect peaks (taken from Fig. 9) as a function of the dose of 300 keV Au ions implanted at LN$_2$ and RT.
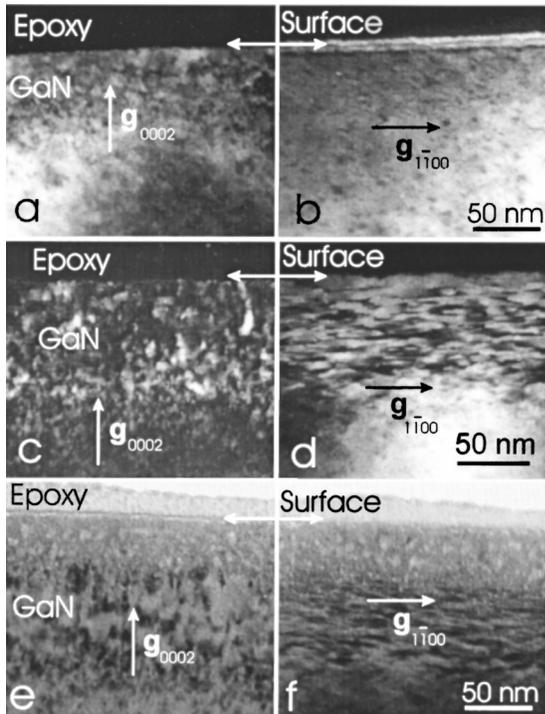
FIG. 10. Cross-sectional dark-field (a)–(d) and bright-field (e),(f) TEM images [(a),(c),(e) $\mathbf{g}=0002^*$ and (b),(d),(f) $\mathbf{g}=1\bar{1}00^*$] of the GaN epilayers bombarded at RT with 300 keV Au ions with a beam flux of $4.4\times10^{12}\,\mathrm{cm}^{-2}\,\mathrm{s}^{-1}$ to doses of $8\times10^{13}\,\mathrm{cm}^{-2}$ (a),(b), $7\times10^{14}\,\mathrm{cm}^{-2}$ (c),(d), and $1.5\times10^{15}\,\mathrm{cm}^{-2}$ (e),(f).

It should be noted that the magnitudes of the surface defect peaks relative to the random level depend on the geometry of RBS/C measurements. For example, it is seen from Fig. 9(a), which shows RBS/C spectra measured with 8° glancing-angle detector geometry, that the surface peak of a sample implanted with 300 keV Au ions at LN_2 temperature to a dose of $3\times10^{14}\,\mathrm{cm}^{-2}$ is below the random level. However, the surface peak of the same sample reaches the random level when measured by RBS/C with about 3° glancing-angle detector geometry to provide a better depth resolution in the near-surface region. This result (obtained also for other selected samples) as well as the TEM data (see Fig. 4) suggest that the strong surface peak in RBS/C spectra arises from a thin amorphous layer on the GaN surface.
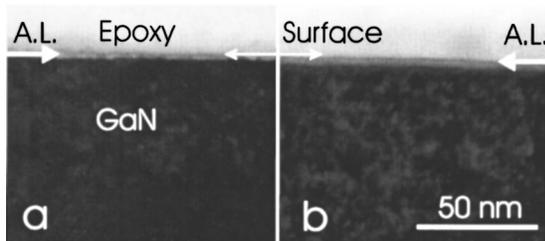
Figure 10 shows TEM images [(a),(c),(e) $\mathbf{g}=0002^*$ and

FIG. 11. Cross-sectional bright-field TEM images of GaN implanted with 300 keV Au ions at RT with a beam flux of $4.4\times10^{12}\,\mathrm{cm}^{-2}\,\mathrm{s}^{-1}$ to a dose of $8\times10^{13}\,\mathrm{cm}^{-2}$ (a) and $7\times10^{14}\,\mathrm{cm}^{-2}$ (b). Amorphous layers (labeled as A. L.) on the GaN surface are clearly demonstrated. The thickness of the surface amorphous layer increases with increasing ion dose.

(b),(d),(f) $\mathbf{g}=1\bar{1}00^*$] taken from GaN implanted at RT with 300 keV Au ions with a beam flux of $4.4\times10^{12}\,\mathrm{cm}^{-2}\,\mathrm{s}^{-1}$ to doses of $8\times10^{13}\,\mathrm{cm}^{-2}$ [Figs. 10(a) and 10(b)], $7\times10^{14}\,\mathrm{cm}^{-2}$ [Figs. 10(c) and 10(d)], and $1.5\times10^{15}\,\mathrm{cm}^{-2}$ [Figs. 10(e) and 10(f)]. Although some defect clusters are seen in the implanted region of the sample bombarded to a dose of $8\times10^{13}\,\mathrm{cm}^{-2}$ [Fig. 10(a)], no planar defects have been revealed by TEM after such a low-dose implantation [Fig. 10(b)]. Again, a strong surface defect peak in the RBS/C spectrum of this sample [Fig. 9(b)] appears to arise from a thin amorphous layer at the GaN surface, as suggested by the bright-field TEM image [see Fig. 11(a)] taken under the same imaging conditions as the images from Fig. 4.

TEM images from the samples implanted to higher doses (7×10^{14} and $1.5\times10^{15}\,\mathrm{cm}^{-2}$) clearly illustrate point-defect clusters (Fig. 10(c,e)) and a band of large planar defects [Figs. 10(d) and 10(f)] produced by heavy ion bombardment. It is also seen from Fig. 10(d) that the region between the surface and the bulk defect peaks is free from planar defects. Additional TEM investigation reveals an amorphous layer on the GaN surface of this sample (a dose of $7\times10^{14}\,\mathrm{cm}^{-2}$), as shown in Fig. 11(b). As expected, the thickness of the surface amorphous layer in this sample (a dose of $7\times10^{14}\,\mathrm{cm}^{-2}$) is larger than the amorphous layer thickness in the sample implanted to a lower dose of $8\times10^{13}\,\mathrm{cm}^{-2}$, as seen from Figs. 11(a) and 11(b). Figures 10(e) and 10(f) illustrate a relatively thick surface amorphous layer (~400 Å thick) in the sample implanted to a dose of $1.5\times10^{15}\,\mathrm{cm}^{-2}$. This result supports the RBS/C data from Fig. 9(b) that, with increasing ion dose, amorphization proceeds layer-by-layer from the surface. Figure 10(f) also shows that, in the saturation regime, the damage in the bulk consists of large planar defects in addition to some defect complexes revealed by Fig. 10(e) taken under different diffraction conditions.

D. Bombardment of GaN capped with SiO_x or Si_xN_y

The formation of an amorphous layer observed at the GaN surface may be due to the effect of preferential loss of nitrogen during ion implantation. To clarify this point, prior to ion bombardment, silicon oxide (SiO_x) or silicon nitride (Si_xN_y) cap layers (~300 Å thick) were deposited on the GaN surface in order to inhibit decomposition of GaN during ion bombardment. RBS/C spectra shown in Figs. 12(a) and 12(b) illustrate the damage buildup in GaN with a SiO_x layer on the GaN surface bombarded at LN_2 [Fig. 12(a)] and RT [Fig. 12(b)] with 450 keV Au ions. Figure 12(c) shows the RBS/C spectra of GaN with a Si_xN_y cap layer on the GaN surface after bombardment with 450 keV Au ions at RT. The Au ion energy of 450 keV was chosen so that, after traveling through an ~300 Å cap layer, the average energy of ions passing through the SiO_x/GaN or Si_xN_y/GaN interface was close to 300 keV. In this case, we can roughly compare these data with the results of 300 keV Au bombardment of GaN without preimplantation capping (Fig. 9).

It is clearly seen from Fig. 12 that capping with either SiO_x or Si_xN_y layers does not eliminate strong surface disordering for both LN_2 and RT bombardment regimes. Therefore, the loss of N from the GaN surface during ion irradiation appears not to be the main reason for preferential
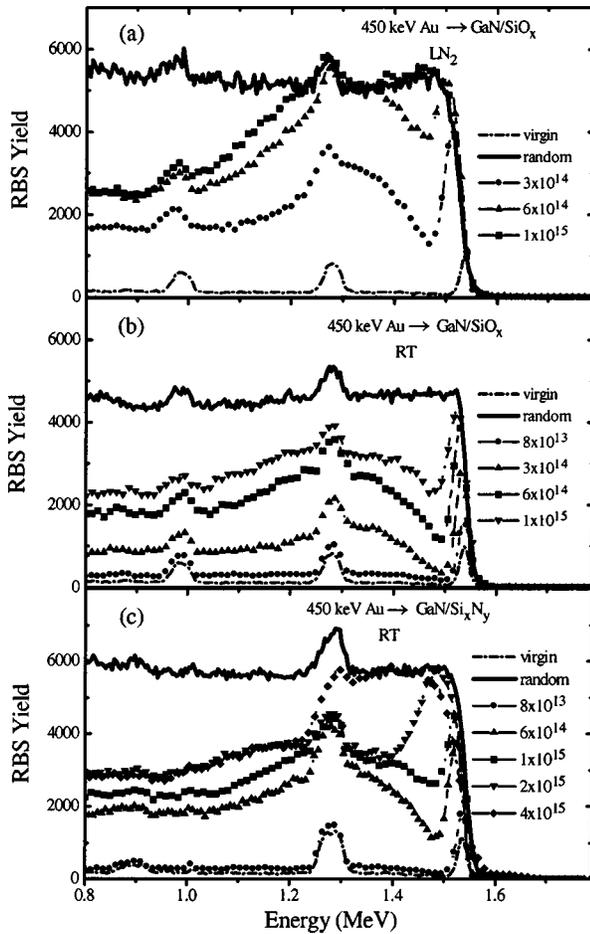
FIG. 12. RBS/C spectra showing the damage buildup in GaN capped with a SiO_x (a),(b) or Si_xN_y (c) layer ~ 300 Å thick. Implantation was carried out with 450 keV Au ions at LN_2 temperature with a beam flux of 3.1×10^{12} cm^{-2} s^{-1} (a) and at RT with a beam flux of 4.4×10^{12} cm^{-2} s^{-1} (b),(c). Implantation doses (in cm^{-2}) are indicated in the figure.

disordering in the near-surface region of GaN and for the formation of a surface amorphous layer, as has also been briefly reported by us previously.[9] The formation mechanism of a surface amorphous layer is revealed more fully by the flux behavior, which is discussed below.

E. Flux effect

Finally, Fig. 13 shows RBS/C spectra illustrating the effect of the beam flux on implantation damage produced by 300 keV Au ion bombardment of GaN at LN_2 [Fig. 13(a)] and RT [Fig. 13(b)]. It is seen that, with increasing beam flux, the magnitude of the bulk defect peak also increases for both LN_2 and RT implantation regimes. However, Fig. 13(b) also shows that, for RT irradiation, the surface defect peak *decreases* in magnitude with increasing beam flux. This *reverse flux effect*, observed also in the case of light ion bombardment of GaN at LN_2 temperature, strongly supports the important role of mobile point defects in the formation and growth of a surface amorphous layer in GaN under ion bombardment, as discussed more fully below. However, Fig. 13(a) shows a normal flux effect (i.e., damage level increases upon increasing beam flux) for the surface defect peak in GaN under irradiation at LN_2 temperature.
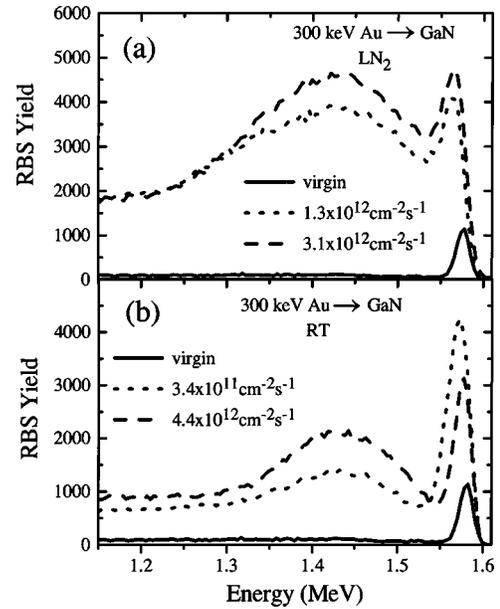

FIG. 13. RBS/C spectra of GaN implanted with 300 keV ions to a dose of 3×10^{14} cm^{-2} at LN_2 (a) and RT (b). The values of beam flux are indicated in the figure. The figure illustrates the reverse and normal flux effects.

IV. DISCUSSION

The above experimental data indicate very strong recovery of ion-generated defects in GaN during ion bombardment even at LN_2 temperature. In contrast to Si or GaAs, GaN is extremely difficult to amorphize by ion bombardment.[18] For example, amorphous layers in Si or GaAs can be created by heavy ion bombardment at RT to doses of the order of 10^{14} cm^{-2}, while GaN remains crystalline to much higher ion doses [see, for example, Figs. 7(b) and 9(b)]. This is a direct consequence of very efficient dynamic annealing processes in GaN during ion bombardment. However, dynamic annealing is never perfect.[18,19] With increasing ion dose, GaN exhibits layer-by-layer amorphization proceeding from the surface as well as the nucleation and growth of a band of extended defects in the bulk.

Very similar behavior has been observed during elevated temperature ion bombardment of Si or GaAs (see, for example, Refs. 14, 15, and 18–22). In fact, at elevated temperatures, Si and GaAs exhibit strong (but also not perfect) dynamic annealing which leads to eventual buildup of radiation damage in the form of extended defects and, ultimately, to amorphization. During elevated temperature ion bombardment of Si or GaAs, amorphization also often proceeds from the surface.

Although ion beam processes in GaN at LN_2 and RT have some similarity with those in Si and GaAs during elevated temperature bombardment, the damage buildup in GaN appears to be even more complex. In the discussion below, we examine a number of defect processes which are plausible in GaN during ion irradiation. Later in this paper, we will briefly return to compare proposed processes in GaN with those discussed in the literature for Si and GaAs.

It should be noted that in the present scenario we do not take into account the chemical effects of implanted carbon and gold atoms on the buildup of radiation damage in GaN.

However, at present, we cannot exclude a possible influence of carbon and gold impurities on the damage accumulation behavior, and this effect requires additional studies.

A. Scenario for defect interaction processes

An energetic ion penetrating through a GaN crystal generates a collision cascade which consists of vacancies in the gallium and nitrogen sublattices (V_{Ga} and V_N), gallium and nitrogen interstitials[23] (Ga_i and N_i), and, presumably, an amorphous zone in the cascade core in the case of heavy ions. Such an amorphous zone is expected to form when the damage level in the collision (sub)cascade volume exceeds some threshold value.[11] However, the damage buildup behavior in GaN under heavy ion bombardment, as illustrated in Figs. 6(b), 7, 9, 12, and 13, strongly suggests that amorphous zones generated by heavy ions are not stable in GaN during ion bombardment at LN_2 temperature and above.

Indeed, if amorphous zones were stable, the gross damage level would be a monotonic function of ion dose due to a gradual accumulation of such amorphous zones until complete amorphization of the implanted region.[10,24] This is in contrast to the highly sigmodal damage buildup experimentally observed even in the case of heavy ion bombardment [Fig. 6(b)]. The RBS/C damage-depth profiles (which have two peaks) and pronounced dynamic annealing during heavy ion bombardment of GaN even at LN_2 temperature also support the fact that the disorder buildup is not governed by accumulation of amorphous zones. On quenching of very dense collision cascades generated by keV heavy ions (such as ^{197}Au), these zones appear to be unstable and anneal via, presumably, both direct thermal and ion-beam-assisted processes.[11,25] However, the possible formation and dynamic annealing of amorphous zones in GaN under different conditions of ion bombardment deserve additional systematic studies [as, for example, has been recently done for GaAs (Ref. 26)].

Ion generated simple point defects (V_{Ga}, V_N, Ga_i, and N_i), which survive after quenching of collisional cascades, therefore, appear to dominate damage buildup during both light and heavy ion bombardment. These defects seem to be mobile even at LN_2 temperature, and most of them experience annihilation. This conclusion directly follows from the fact that the experimentally measured amount of lattice disorder is much less than that predicted by calculations (such as the TRIM code[16]) which take into account only collisional processes and neglect defect diffusion and annihilation.[18] Such a substantial annihilation may indicate a high rate of the direct recombination processes: $V_{Ga}+Ga_i \rightarrow 0$, $V_N+N_i \rightarrow 0$. Nevertheless, indirect annihilation processes (recombination of a vacancy [interstitial] via trapping at an interstitial [vacancy] complex) cannot be excluded. Dynamic annealing may also result in the formation of antisite defects ($V_{Ga} + N_i \rightarrow N_{Ga}$; $V_N + Ga_i \rightarrow Ga_N$).

The initial sluggish growth of the gross damage for low ion doses,[17] observed in Figs. 1, 6, 7, and 9, is, therefore, due to a considerable recombination of ion-generated point defects. However, defect annihilation is not perfect, and point-defect clusters (presumably complexes of vacancies and/or interstitials, as well as defect-impurity complexes) appear with further increasing ion dose, as indicated by TEM and RBS/C data. It is also reasonable to expect dynamic annealing of these complexes via interaction with ion-generated mobile point defects. For example, a vacancy cluster is expected to anneal via trapping of mobile interstitials. This process, on the other hand, represents an example of a two-step (indirect) annihilation of a Frenkel pair: first, trapping of a vacancy (interstitial) at a complex; second, recombination of this quiescent vacancy (interstitial) with a mobile interstitial (vacancy).

TEM investigation reveals that defect recombination and formation of defect complexes are not the only processes taking place in GaN during ion bombardment (see Figs. 3, 8, and 10). A band of planar defects in the crystal bulk also nucleates with increasing ion dose at both LN_2 and RT bombardment with light or heavy ions. The microscopic structure and formation mechanism of these planar defects are not understood at present and warrant additional systematic studies.

The defect processes during ion bombardment of GaN are also complicated by the influence of the GaN surface (or GaN/capping layer interface). Indeed, the GaN surface appears to represent an effective sink for migrating point defects. The flux behavior (see Fig. 13) suggests that mobile point defects play an important role in the formation and growth of the surface amorphous layer. Indeed, a normal flux effect (i.e., with increasing beam flux, the damage level also increases) is observed for the bulk peak of damage (see Fig. 13). This is consistent with the current understanding of implantation damage buildup in semiconductors under implantation conditions when substantial dynamic annealing of radiation defects takes place (see, for example, Refs. 10, 14, 15, 18, and 19). An increase in the beam flux decreases the average time interval between collision cascades which spatially overlap. Such an increase in the generation rate of point defects with increasing beam flux enhances the rate of interactions between mobile defects and, therefore, enhances the formation of defect complexes. However, Fig. 13(b) also shows that the surface defect peak decreases in magnitude with increasing beam flux. This reverse flux effect can be qualitatively explained in terms of the competition between defect trapping and migration processes. Indeed, an increase in the beam flux enhances the formation of defect complexes in the crystal bulk. As a result, fewer point defects generated in this region can reach the surface.

The influence of the surface on the point defects generated in the crystal bulk is determined by the effective mobility of defects and, of course, by the distance between the surface and the region where these defects are generated. Figures 7 and 9 show that the main features of damage buildup remain the same upon increasing the energy of Au ions from 100 to 300 keV. However, an additional systematic study of the dependence of damage buildup on the distance between the surface and the maximum of the nuclear energy loss profile is highly desirable.

The well-known effect of local material stoichiometric imbalance in the collision cascade volume[27] may also affect damage accumulation and annealing. Indeed, in the case of a compound semiconductor, an excess concentration of the heavier element exists at shallow depth, while the region at greater depth is enriched with atoms of the lighter element. Calculations show that such stoichiometric disturbances are

greatest when the mass ratio of the constituent elements of the semiconductor is high, and when the ion mass is large.[27] Therefore, for the case of implantation of ^{197}Au ions into GaN—a material with a large difference in the masses of constituent elements (^{70}Ga and ^{14}N)—the effect of local stoichiometric imbalance under bombardment should be taken into account.

However, the final local stoichiometry after ion bombardment depends not only on the ballistic collisional processes but also on defect migration. The stoichiometric disturbances may be effectively repaired via defect diffusion and dynamic annealing, processes which are rather effective in GaN at LN$_2$ temperature and above. Because such local stoichiometric imbalance of GaN could significantly affect disorder removal during post-implantation annealing, additional systematic studies of this effect are desirable and may have significant implications for a successful application of ion beams for the fabrication of GaN-based devices.

The effect of local stoichiometric imbalance may account for the distorted shape of the RBS/C channeling and random spectra illustrated in Fig. 9 for GaN heavily damaged by Au ions. For example, Fig. 9(a) shows that both channeling and random spectra of the sample implanted with 300 keV Au ions to a dose of 1×10^{15} cm^{-2} at LN$_2$ temperature have a ''shoulder'' with a decreased RBS/C yield in the ion end-of-range region and increased yield near the GaN surface. This indicates that the near-surface region of GaN is enriched with Ga atoms, while the region at greater depth has a Ga deficiency. Compared to LN$_2$ temperature, the spectra of GaN implanted with 300 keV ions at RT have a less pronounced distortion, as indicated in Fig. 9(b).

Such a distortion in RBS/C spectra does not seem to be the result of the introduction of a high concentration of Au atoms into the GaN lattice because of the relatively small ion doses used ($\sim 1 \times 10^{15}$ cm^{-2}), where the Au concentration is $\leqslant 1$ atomic percent. This conclusion is also supported by the facts that (i) the magnitude of such a distortion does not change with increasing ion dose from 6×10^{14} to 1×10^{15} cm^{-2} for LN$_2$ temperature bombardment [see Fig. 9(a)], and (ii) this distortion is larger for LN$_2$ temperature implantation than for irradiation at RT although ion doses for RT are larger [see Figs. 9(a) and 9(b)]. Thus, with increasing implantation temperature, stoichiometric disturbances are more effectively repaired, owing to enhanced defect diffusion and dynamic annealing processes.

In addition to local material stoichiometric imbalance produced by heavy ion implantation of GaN, loss of nitrogen from the GaN surface during ion bombardment also appears to contribute to the distortion of the near-surface region in the RBS/C spectra, as has been reported by us previously.[9] In particular, the well-known effect of preferential sputtering,[28] which may significantly change the composition of the near-surface region of a compound semiconductor, may be important, given the high ion doses used in this study. However, based on collisional processes alone,[29] the effect of preferential sputtering cannot account for the large effects in Fig. 9.

A further important mechanism which may significantly affect dynamic annealing and hence the damage buildup in GaN is worth mentioning. Indeed, it is well known that vacancies and interstitials are spatially separated in a collision cascade,[28] with an interstitial excess at the ion end-of-range

and a vacancy excess closer to the surface. The effect of such a spatial separation of vacancies and interstitials for each collision cascade is expected to become more pronounced with increasing ion dose. As a result, this effect could also be important in controlling damage accumulation in GaN, given the high ion doses required for amorphization of GaN.

Finally, a comment should be made on the possibility of developing a quantitative model for damage buildup in GaN. It is clear that all ''traditional'' quantitative models[10,24] can be applied only when the rate of dynamic annealing is considerably lower than the defect production rate, which is not the case even for heavy ion bombardment of GaN at LN$_2$ temperature. At present, the development of a model which takes into account elemental defect processes and dynamic annealing in GaN during ion bombardment appears to be a rather difficult task due to a very limited understanding of these processes. It is clear that additional experimental studies are necessary before a satisfactory quantitative model for damage buildup in GaN can be developed.

B. Bombardment at LN$_2$ temperature

Based on the above discussion, we can qualitatively explain the damage buildup observed in GaN under ion bombardment at LN$_2$ temperature. Very similar damage buildup behavior at LN$_2$ temperature has been observed in both cases of light and heavy ion bombardment. Therefore, these two cases are discussed below together.

At low doses,[17] ion-generated mobile point defects exhibit substantial annihilation, while some defects are trapped at the surface, giving rise to the strong surface peak in RBS/C spectra [Figs. 1(a), 7(a), and 9(a)] via, presumably, layer-by-layer amorphization proceeding from the GaN surface, as indicated by an appearance of an amorphous layer at the GaN surface (see Fig. 4).

Despite effective recombination of mobile defects, defect complexes accumulate with increasing ion dose. In addition, a band of planar defects nucleates in the bulk region [Figs. 3(b), 8(c), and 8(d)]. Then, with a further increase in the ion dose, the damage in the GaN bulk exhibits a very rapid growth from a low level to amorphization, as suggested by the RBS/C yield reaching the random level in Figs. 1(a), 7(a), and 9(a). This rapid damage buildup (or a strong sigmodality of the damage-dose function) is a characteristic feature of nucleation-limited amorphization, where the initial stage of ion bombardment results in the formation of ''nucleation sites'' for amorphization.[18] When such ''nucleation sites'' are formed, subsequent irradiation of a predamaged crystal leads to a very fast increase in the damage level with increasing ion dose.

A correlation between RBS/C and TEM data [see Figs. 7(a), 8(c), and 8(d)] indicates that the onset of the fast growth of damage with increasing ion dose (as observed by RBS/C) coincides with the formation of the planar defects (as observed by TEM). This fact may suggest that the planar defects are plausible candidates for the ''nucleation sites'' of amorphization. When these planar defects form, an increase in the ion dose results in very fast damage accumulation. However, further study is necessary to ultimately ascertain whether the band of planar defects acts as a ''nucleation site'' for amorphization during ion bombardment at LN$_2$ temperature.

C. Bombardment at room temperature

The rate of all thermally activated defect processes should be enhanced at RT compared to LN$_2$ temperature irradiation. The scenario at RT, as compared to bombardment at LN$_2$ temperature, becomes more complicated. Because different damage buildup behavior has been observed for RT bombardment with light and heavy ions, these two cases are considered separately.

1. Light ions

Figures 1(b) and 6(a) show that for RT bombardment with 40 keV C ions, after initial relatively fast growth, the surface peak exhibits plateauing in the dose range from 1×10^{16} to 3×10^{16} cm^{-2}. This rather unexpected plateauing effect can be tentatively explained as follows. Damage accumulation in the bulk defect peak region may become more efficient when the ''nucleation sites'' for amorphization (presumably, planar defects) are fully formed. Such efficient defect trapping is supported by a highly sigmodal damage buildup in the crystal bulk with increasing ion dose [see Fig. 6(a)]. After the ''nucleation sites''form in the bulk, fewer defects generated by an ion beam can reach the surface from the bulk, which may be the reason for the observed plateauing of the surface defect peak. However, for higher doses ($>3 \times 10^{16}$ cm^{-2}), as soon as a buried amorphous layer forms in the bulk (as suggested by the channeling RBS/C yield reaching the random level), two amorphous/crystalline interfaces of the buried and surface amorphous layers seem to have similar efficiency to trap mobile defects. These two amorphous layers appear to grow layer-by-layer and ultimately join together with a further increase in the dose, as seen from Fig. 1(b). The buried amorphous layer expands faster than the surface layer since the defect generation rate in the bulk is higher than that near the surface.

An increased (presumably, trap-limited) defect mobility at RT compared to LN$_2$ temperature bombardment is also supported by an apparent shift of the maximum of the bulk defect peak (to greater depths) with increasing implantation temperature. For example, the damage peak at LN$_2$ temperature for a dose of 8×10^{15} cm^{-2} is close to $\sim$470 Å, but the depth of the damage peak for a dose of 2×10^{16} cm^{-2} at RT is near $\sim$620 Å, as shown in Figs. 1(a) and 1(b). Such behavior has previously been observed for elevated temperature bombardment of Si, where disorder is found to buildup beyond the maximum of the nuclear energy deposition distribution at so-called end-of-range defects.[21] These end-of-range defects in Si consist of interstitial-based clusters and small loops which arise from the well-known spatial separation of vacancies and interstitials in a collision cascade, with an interstitial excess at the ion end of range and a vacancy excess closer to the surface. In Si, under strong dynamic annealing conditions, mobile defects are preferentially trapped at the surface or in the end-of-range region where the interstitial excess coalesces. A somewhat similar explanation might be proposed for the RT behavior observed in GaN. Strong defect annihilation and increased defect mobility may lead to a dominant trapping of defects both at the surface and at the end of range for 40 keV C ions implanted into GaN. However, we cannot exclude the role of carbon (i.e., trapping of point defects by carbon atoms) in this process since the carbon dose is very high during damage buildup at RT.

Finally, a comment could be made on the apparently increased damage produced at RT compared to LN$_2$ temperature light ion bombardment to low doses (see Fig. 5). This interesting result may be qualitatively explained based on the fact that an increase in implantation temperature leads to an increase in the rate of all thermally activated point-defect processes (defect diffusion, direct and indirect annihilation, formation of complexes, trapping of free defects by defect complexes and impurities, etc.). The nature of ''stable'' defect complexes formed at RT during dynamic annealing may, as a consequence, result in a higher level of residual disorder. However, at present, further experimental work is necessary to identify the most plausible mechanism for this somewhat odd temperature-dependent effect.

2. Heavy ions

Figures 7(b) and 9(b) show that, for low doses of Au ions ($\sim$8$\times$10^{13} cm^{-2}), the damage buildup at RT is very similar to that during LN$_2$ temperature irradiation. Most of the ion-generated defects annihilate, while some of them trap at the surface and, presumably, form a surface amorphous layer (as seen in TEM images in Fig. 11), giving rise to the strong surface peak in the RBS/C spectra shown in Figs. 7(b) and 9(b).

An increased effective mobility of point defects at RT, as compared to LN$_2$ temperature, is supported by the fact that, for low ion doses, the surface defect peak for RT bombardment is larger than that for irradiation at LN$_2$ temperature, as indicated in Fig. 6(b). This fact, as well as the reverse flux effect on the surface defect peak [see Fig. 13(b)], might suggest that, during 300 keV Au ion bombardment at RT, point defects generated in the whole implantation region (up to $\sim$900 Å from the GaN surface) contribute to the formation of the surface amorphous layer. In contrast, the normal flux effect (i.e., damage level increases upon increasing the beam flux) for the surface defect peak for 300 keV Au ion bombardment at LN$_2$ temperature [Fig. 13(a)] may be attributed to smaller effective diffusion lengths of point defects, as compared to ion irradiation at RT.

Again, as in the case of LN$_2$ temperature bombardment, defect annihilation is not perfect, and, with increasing ion dose, in addition to layer-by-layer amorphization proceeding from the surface, point-defect complexes are formed as well as a band of planar defects in the GaN crystal bulk (see Fig. 10). With further increasing ion dose, Figs. 7(b) and 9(b) indicate that the damage level (as measured by RBS/C) in the GaN bulk region saturates below the random level, and layer-by-layer amorphization proceeds from the GaN surface (see Fig. 10). For this saturation regime, the disorder in the bulk consists of a band of planar defects as revealed by TEM [Figs. 10(d) and 10(f)]. Figures 9(b), 10(d), and 10(f) also show that the band of planar defects broadens with further increasing dose. For Au ion implantation, this band of planar defects does not amorphize independently of the surface amorphous layer (as has been observed for light ions) but, rather, is consumed by the advancing surface amorphous layer.

The above effect of bulk damage saturation represents an example in which the processes of defect production and removal are balanced in some region of a crystal. It should

be noted that the existence of such a saturation regime does not necessarily require that all point defects generated by an ion beam in some region of a sample exhibit perfect annihilation. Indeed, point defects produced by ion irradiation in the region with planar defects might not increase the density of such extended defects but, rather, lead to the expansion of the planar defect band. At present, it is difficult to propose an unequivocal microscopic mechanism to account for the existence of the saturation regime and the extension of the band of planar defects. However, this effect may be attributed to (i) the enhanced annihilation of point defects within the region containing a saturation density of planar defects and/or to (ii) energetically favorable processes (possibly stress-induced) relating to defect annihilation and/or agglomeration after the nucleation of a band of planar defects. Additional-studies are highly desirable to understand the evolution and saturation of defects in GaN during ion bombardment.

D. Surface defect peak

A comment on the unusually strong surface defect peak observed in GaN should be made. A thin surface amorphous layer has been observed in GaN implanted to a relatively low dose of 300 keV Au ions at LN_2 temperature, as shown in Fig. 11(a). In addition, Fig. 4(a) clearly indicates the presence of a surface amorphous layer for a relatively high dose (8×10^{15} cm^{-2}) of 40 keV C ions implanted at LN_2 temperature. Nevertheless, it is interesting to ascertain whether or not the surface defect peak measured by RBS/C for lower doses results from an amorphous layer. TEM investigation on samples implanted with 40 keV C ions with a beam flux of 1.4×10^{13} cm^{-2} s^{-1} to a dose of 1×10^{15} cm^{-2} at LN_2 and RT did not reveal any amorphous layer on the GaN surface. Therefore, the strong surface peak in RBS/C spectra of low dose irradiated GaN samples seems to arise from the lattice reconstruction of the first several monatomic layers on the GaN surface due to, presumably, (i) accumulation of point defects at the GaN surface, (ii) ion-produced preferential loss of N,[9,30] and/or (iii) recoil implantation of the impurities from a thin layer of surface contamination. Such a very thin near-surface layer of reconstructed lattice may act as a precursor for a surface amorphous layer which appears with increasing ion dose. Additional work is desirable to study damage of the GaN surface produced by light ion bombardment.[17]

Finally, it is worth mentioning that the surface peak of disorder produced by ion bombardment of semiconductors is not a new effect. This effect was studied in the 1970s by different experimental techniques (such as RBS/C, electron diffraction, electron paramagnetic resonance, and electron backscattering) for the case of ion implantation into Si (see, for example, Refs. 31–36). In addition, the nucleation of amorphous layers in Si preferentially at the surface has been observed during elevated temperature bombardment.[22] The surface peak of damage has also been studied in Ge and GaAs,[37] and, very recently, ion-bombardment-induced anomalous surface disordering in Si has received new interest due to important applications of low-energy ion beams for the formation of very shallow junctions in Si.[38,39]

The results of previous studies on Si, Ge, and GaAs (Refs. 21, 22, and 31–37) also suggest that the origin of the surface defect peak can be attributed to an amorphous layer at the semiconductor surface, presumably formed due to trapping of migrating point defects by the surface. In the case of GaN, the data presented above and elsewhere[9] show that the strong surface peak of disorder also often arises from an amorphous layer on the GaN surface, as indicated by TEM. In addition, the flux behavior of damage strongly supports the fact that the surface defect peak in GaN may be attributed to trapping of mobile point defects by the GaN surface.

E. Comparison of light and heavy ion bombardment

A brief comparison between damage buildup in GaN under heavy and light ion bombardment can be made. The following similarities between these two irradiation regimes are evident.

(i) Substantial dynamic annealing of ion-produced defects has been observed for both regimes at LN_2 and RT.

(ii) For both irradiation regimes, the damage-depth profile, as measured by RBS/C, has two peaks—the surface and bulk defect peaks. This feature has been attributed to high defect mobility and high efficiency of the GaN surface to trap migrating point defects.

(iii) In both cases, a band of planar defects nucleates in the crystal bulk with increasing ion dose. However, the size of such planar defects appears to depend on implant conditions.

(iv) Similar damage buildup behavior at LN_2 temperature has been observed in both cases of light and heavy ion bombardment.

However, the following differences between light and heavy ion bombardment regimes are worth mentioning.

(i) Completely different damage accumulation behavior has been observed for RT bombardment by light (^{12}C) and heavy (^{197}Au) ions. No damage saturation in the GaN bulk during irradiation with light ions has been observed, as measured by RBS/C. This fact may be explained by the difference in the defects formed during bombardment with light and heavy ions (for example, different size of planar defects). However, the chemical effects of implanted carbon and/or gold atoms may also influence the buildup of radiation damage in GaN, and this requires additional study.

(ii) A comparison of the disorder levels, as measured by RBS/C, with the results of TRIM calculations[16] shows that the defect annihilation efficiency is higher for light ion bombardment than that for irradiation with heavy ions. This result is consistent with the fact that the defect generation *rate* is larger in the case of heavy ion bombardment. Such an increase in the generation rate of defects enhances the rate of interaction between mobile defects, and, consequently, promotes the formation of defect complexes.[10,18,19]

(iii) No reverse flux effect on the surface defect peak has been observed for LN_2 temperature bombardment with heavy ions [see Fig. 13(a)], while a small reverse flux effect has been observed in the case of light ion bombardment at LN_2 temperature (figure is not shown). This result may indicate a lower effective mobility of point defects for heavy ion bombardment due to denser collision cascades and, hence, enhanced local defect interaction, as compared to the case of irradiation with light ions.

F. Comparison of damage buildup in GaN with that in Si and GaAs

Finally, we make a brief comparison of implantation disorder buildup in GaN with that in much better studied semiconductors—Si and GaAs. As alluded to earlier, some features of damage buildup in GaN at LN$_2$ temperature resemble those occurring in Si or GaAs during elevated-temperature ion bombardment. Indeed, during elevated-temperature ion bombardment of these latter materials, when dynamic annealing of ion-generated defects is strong, damage accumulation proceeds via the formation of an array of extended defects, as has been reviewed elsewhere.[18,19] These extended defects in Si or GaAs are usually tangles of dislocations, and their density increases with increasing ion dose. This causes a continuous rise in the total energy of the system until the system collapses into the energetically more preferable amorphous state.[40] In addition, in Si or GaAs bombarded at an elevated temperature, layer-by-layer amorphization can proceed from the surface. In this case, the surface acts as a ''nucleation site'' for amorphization.

The scenario for amorphization in GaN under ion bombardment at LN$_2$ temperature appears to be qualitatively similar to that in Si or GaAs at elevated implant temperature. Indeed, damage evolution in GaN proceeds via the formation of a band of extended defects. The surface of GaN also acts as a ''nucleation site'' for amorphization. However, the ion-produced extended defects in GaN consist of a regular array of planar defects, not dislocation tangles as in Si or GaAs. Moreover, the presence of a saturation regime during RT bombardment of GaN with heavy ions may suggest that the process of amorphization in GaN is more complex than that in Si or GaAs during elevated-temperature bombardment. Indeed, in addition to the possible chemical effects of implanted atoms, amorphization of GaN seems to be stimulated by the processes of local stoichiometric imbalance, which should become pronounced for high ion doses. This may explain why amorphous zones presumably generated in dense collisional cascades produced by heavy ions appear to be unstable in GaN, whereas surface and buried amorphous layers can be nucleated for very high ion doses. However, it is obvious that, at present, much more experimental work is necessary for a deeper understanding of amorphization mechanisms in GaN.

V. CONCLUSIONS

In conclusion, damage buildup and amorphization behavior in GaN under keV light (^{12}C) and heavy (^{197}Au) ion bombardment at LN$_2$ and room temperatures have been stud-ied by a combination of RBS/C and TEM techniques. The effect of beam flux on radiation damage in GaN has been reported. The experimental data presented point to a complex role of mobile, irradiation-induced defects in controlling damage accumulation. The data indicate that significant annihilation of damage occurs even during heavy ion bombardment at LN$_2$ temperature. Point defects, which survive after quenching of collisional cascades, appear to be the dominant type of defects controlling disorder accumulation during ion bombardment at LN$_2$ temperature and above.

With increasing dose of light or heavy ions, amorphization starts from the GaN surface although the surface is well separated from the maximum of the nuclear energy deposition profile. As a result, experimentally measured damage-depth profiles in GaN after light or heavy ion bombardment at LN$_2$ or RT significantly depart from those predicted by TRIM calculations,[16] which take into account only collisional processes and neglect dynamic annealing. RBS/C spectra have a strong surface peak which arises from an amorphous layer at the GaN surface. The origin of such an amorphous layer is attributed to the trapping of migrating point defects by the GaN surface.

Damage buildup is highly sigmodal during LN$_2$ temperature bombardment with light or heavy ions. For heavy ion irradiation at RT, the damage in the bulk region saturates at a level lower than the random level, as measured by RBS/C. A band of planar defects nucleates in the GaN bulk region for both LN$_2$ and RT implantation regimes. The planar defects have been assumed to provide a ''nucleation site'' for amorphization with further increasing ion dose during LN$_2$ temperature irradiation. However, it appears energetically favorable for such planar defects to grow rather than to nucleate an amorphous phase for Au ion irradiation at RT. A number of possible damage processes, which may take place in GaN under ion bombardment, have been discussed. The somewhat unexpected behavior of damage buildup has been qualitatively explained based on complex dynamic annealing processes. Finally, this study shows again that GaN is not only a material with promising device applications but is also one which exhibits rather interesting defect-controlled disordering behavior under ion bombardment.

*Email address: sok109@rsphysse.anu.edu.au

[1] See, for example, recent reviews S. J. Pearton, J. C. Zolper, R. J. Shul, and F. Ren, J. Appl. Phys. **86**, 1 (1999); S. C. Jain, M. Willander, J. Narayan, and R. Van Overstraeten, *ibid.* **87**, 965 (2000).

[2] H. H. Tan, J. S. Williams, J. Zou, D. J. Cockayne, S. J. Pearton, and R. A. Stall, Appl. Phys. Lett. **69**, 2364 (1996).

[3] N. Parikh, A. Suvkhanov, M. Lioubtchenko, E. Carlson, M. Bremser, D. Bray, R. Davis, and J. Hunn, Nucl. Instrum. Methods Phys. Res. B **127/128**, 463 (1997).

[4] A. Suvkhanov, J. Hunn, W. Wu, D. Thomson, K. Price, N. Parikh, E. Irene, R. F. Davis, and L. Krasnobaev, in *Wide-Bandgap Semiconductors for High Power, High Frequency and High Temperature*, edited by S. DenBaars, J. Palmour, M. S. Shur, and M. Spencer, Mater. Res. Soc. Symp. Proc. No. 512 (Materials Research Society, Warrendale, 1998), p. 475.

[5] H. H. Tan, J. S. Williams, J. Zou, D. J. Cockayne, S. J. Pearton, J. C. Zolper, and R. A. Stall, Appl. Phys. Lett. **72**, 1190 (1998).

[6] C. Liu, B. Mensching, M. Zeitler, K. Volz, and B. Rauschenbach, Phys. Rev. B **57**, 2530 (1998).

[7] W. Jiang, W. J. Weber, S. Thevuthasan, G. J. Exarhos, and B. J. Bozlee, MRS Internet J. Nitride Semicond. Res. **4S1**, G6.15 (1999).

[8] W. R. Wampler and S. M. Myers, MRS Internet J. Nitride Semicond. Res. **4S1**, G3.73 (1999).

[9] S. O. Kucheyev, J. S. Williams, C. Jagadish, G. Li, and S. J. Pearton, Appl. Phys. Lett. **76**, 3899 (2000).

[10] J. F. Gibbons, Proc. IEEE **60**, 1062 (1972).

[11] For a more detailed discussion of amorphous zone formation in semiconductors, see, for example, D. J. Mazey, R. S. Nelson, and R. S. Barnes, Philos. Mag. **17**, 1145 (1968); L. M. Howe and M. H. Rainville, Nucl. Instrum. Methods Phys. Res. B **19/20**, 61 (1987); J. A. Davies, in *Ion Implantation and Beam Processing*, edited by J. S. Williams and J. M. Poate (Academic, Sydney, 1984).

[12] W.-K. Chu, J. W. Mayer, and M.-A. Nicolet, *Backscattering Spectrometry* (Academic, Orlando, 1978).

[13] J. S. Williams, M. Conway, J. A. Davies, M. Petravic, H. H. Tan, and J. Wong-Leung, Nucl. Instrum. Methods Phys. Res. B **136–138**, 453 (1998).

[14] R. A. Brown and J. S. Williams, J. Appl. Phys. **81**, 7681 (1997).

[15] J. S. Williams, R. D. Goldberg, M. Petravic, and Z. Rao, Nucl. Instrum. Methods Phys. Res. B **84**, 199 (1994).

[16] J. P. Biersack and L. G. Haggmark, Nucl. Instrum. Methods **174**, 257 (1980).

[17] We consider the value of dose to be low or high based on the damage level produced.

[18] J. S. Williams, Mater. Sci. Eng., A **253**, 8 (1998).

[19] J. S. Williams, Trans. Mater. Res. Soc. Jpn. **17**, 417 (1994).

[20] R. A. Brown and J. S. Williams, Phys. Rev. B **55**, 12 852 (1997).

[21] R. D. Goldberg, J. S. Williams, and R. G. Elliman, Phys. Rev. Lett. **82**, 771 (1999).

[22] R. D. Goldberg, J. S. Williams, and R. G. Elliman, in *Materials Synthesis and Processing Using Ion Beams*, edited by R. J. Culbertson, O. W. Holland, K. S. Jones, and K. Maex, Mater. Res. Soc. Symp. Proc. No. 316 (Materials Research Society, Pittsburgh, 1994), p. 259.

[23] In our simple scenario, we do not distinguish between interstitials of different symmetry.

[24] For a brief review of the models for damage buildup in semiconductors, see, for example, A. I. Titov and G. Carter, Nucl. Instrum. Methods Phys. Res. B **119**, 491 (1996).

[25] R. S. Nelson, Radiat. Eff. **32**, 19 (1977).

[26] M. W. Bench, I. M. Robertson, M. A. Kirk, and I. Jenčič, J. Appl. Phys. **87**, 49 (2000).

[27] See, for example, L. A. Christel and J. F. Gibbons, J. Appl. Phys. **52**, 5050 (1981).

[28] See, for example, M. Nastashi, J. W. Mayer, and J. K. Hirvonen, *Ion-Solid Interactions: Fundamentals and Applications* (Cambridge University Press, Cambridge, 1996).

[29] H. H. Andersen, in *Ion Implantation and Beam Processing*, edited by J. S. Williams and J. M. Poate (Academic, Sydney, 1984).

[30] C. R. Eddy, Jr. and B. Molnar, J. Electron. Mater. **28**, 314 (1999).

[31] A. I. Gerasimov, E. I. Zorin, P. V. Pavlov, and D. I. Tetelbaum, Phys. Status Solidi A **12**, 679 (1972).

[32] H. J. Pabst and D. W. Palmer, Inst. Phys. Conf. Ser. **16**, 438 (1973).

[33] V. N. Gashtol'd, N. N. Gerasimenko, A. V. Dvurechenski, and L. S. Smirnov, Fiz. Tverd. Tela (Leningrad) **9**, 835 (1975) [Sov. Phys. Semicond. **9**, 551 (1975)].

[34] I. A. Abroyan, A. I. Titov, and A. V. Khlebalkin, Fiz. Tverd. Tela (Leningrad) **11**, 1204 (1977) [Sov. Phys. Semicond. **11**, 712 (1977)].

[35] W. H. Kool, H. E. Roosendaal, L. W. Wiggers, and F. W. Saris, Radiat. Eff. **36**, 41 (1978).

[36] A. I. Titov, C. E. Christodoulides, G. Carter, and M. J. Nobes, Radiat. Eff. **41**, 107 (1979).

[37] I. A. Abroyan, V. S. Belyakov, and A. I. Titov, *Proceedings of the IX All-Russian Conference on Interactions of Atomic Particles with Solids* (Moscow Engineering and Physical Institute, Moscow, 1989), Vol. 2, p. 81.

[38] T. Lohner, M. Fried, N. Q. Khanh, P. Petrik, H. Wormeester, and M. A. El-Sherbiny, Nucl. Instrum. Methods Phys. Res. B **147**, 90 (1999).

[39] K. Kimura, A. Agarwal, H. Toyofuku, K. Nakajima, and H.-J. Gossmann, Nucl. Instrum. Methods Phys. Res. B **148**, 284 (1999).

[40] M. L. Swanson, J. R. Parsons, and C. W. Hoelke, Radiat. Eff. **9**, 249 (1971).